Spring 5-2-2011

A Generalized Flow Regime Diagram for Fluid-Solid Vertical Transport

Xiaotao T. Bi
University of British Columbia, xbi@chml.ubc.ca

A GENERALIZED FLOW REGIME DIAGRAM FOR FLUID-SOLID VERTICAL TRANSPORT

Xiaotao T. Bi
Fluidization Research Centre
Department of Chemical and Biological Engineering
The University of British Columbia, Vancouver, Canada

ABSTRACT

An ideal generalized flow regime diagram was proposed for fluid-solids vertical transport systems with no bottom and top restrictions. Such an ideal flow regime diagram was further extended to shed light onto the understanding of the flow regimes and instabilities encountered in bottom- restricted bubbling and circulating fluidized bed systems.

INTRODUCTION

Flow patterns and flow regimes in gas-solids two-phase fluidization and vertical flow systems have attracted a great attention in the multiphase research community since the 1940s. A number of flow regime maps have been proposed to distinguish different unique flow patterns. Although it has been commonly agreed that there exist distinct flow patterns in gas-solids fluidized beds and vertical transport lines, such as the bubbling and slugging fluidization and dilute phase transport based on extensive research from 1940s to 1960s. Controversies still exist on the existence of turbulent fluidization, which was first proposed in late 1960s, fast fluidization, which was first proposed in late 1970s. The transition from pneumatic conveying to fast fluidization or dense suspension upflow is still not well defined, as reflected in the debates on the definition of choking in Fludization X in Beijing and CFB-7 in Naragra Falls. Further work on this topic is warranted in order to develop a generalized flow regime diagram for the flow pattern identification. In this work, attempt was made to elucidate the flow patterns in free or non-restricted gas-solids vertical flow systems in hope that such an analysis will shed some light on the understanding of the bottom-restricted fluidized bed systems and the dense suspension upflow system in which the solids feeding system is coupled with the flow in the riser.

FLOW PATTERNS IN FREE GAS-SOLIDS VERTICAL FLOW SYSTEMS

In gas-solids vertical flow systems with gas flowing upward, particles can travel up or down, giving rise to two possible flow modes: co-current upflow and counter-current flow. The termination of counter-current flow occurs when solids can no longer fall downward (i.e. at the ***flooding*** point) and the gas-solids co-current upflow ceases when the gas velocity is lower than particle terminal settling velocity.

If we feed solids from the middle section into a vertical tube with open top and bottom in which gas is flowing from bottom to top, both co-current upward flow in the upper section above the feeding point and counter-current flow in the lower section below the feeding point are possible depending on the gas velocity and the solids feeding rate. At a gas velocity lower than the particle terminal velocity, all feed particles will fall downward at a low feed rate, forming a counter-current flow in the lower section of the tube and a single-phase gas flow in the upper section, as shown in Figure 1. However, with the increase in solids feed rate, flooding will be reached when particles discharge rate from the bottom end of the tube becomes smaller than the solids feed rate. As a result, solids start to build up upward into the upper section, forming a dense fluidized bed in the upper section. This flooding phenomenon is in analogy to the flooding in gas-liquid counter-flow systems.

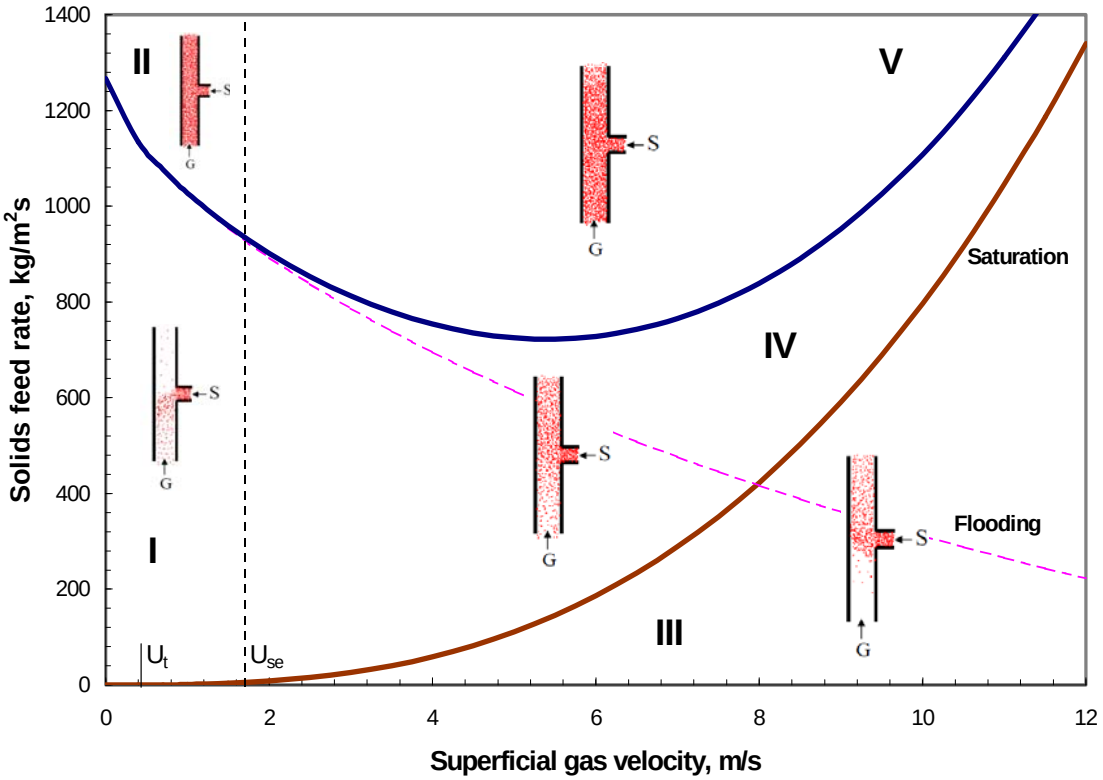

Figure 1. A flow regime diagram for non-restricted vertical transport lines. FCC particles in ambient air: mean particle size, 60 μm; particle density, 1800 kg/m^3.

Let us now consider the case when the gas velocity in the tube is higher than the particle terminal settling velocity. At a low solids feed rate all fed particles are carried upward giving a co-current upward flow in the upper section, and a single-phase gas flow in the lower section, shown in Figure 1. When the solids feed rate is increased to such an extent that the solids feed rate exceeds the saturation particle carrying capacity of the gas, excess amount of particles will fall downward and leave the tube from the bottom, forming a counter-current flow in the lower section as well as a co-current upward flow in the upper section. If the solids feed rate is further increased to such an extent that the downflowing particle rate exceeds the flooding rate which corresponds to the maximum discharge rate from the bottom end of the column, a

dense suspension starts to build up above the solids feed point, forming a co-current dense suspension upflow in the upper section and a flooded counter-current flow in the lower section.

A flow regime diagram for a given vertical tube, gas and particle properties can be constructed based on the flooding velocity and the gas velocity corresponding to the saturation carrying capacity, estimated from two correlations:

Equation (1) from Papa and Zenz [1], which was modified from the Sherwood equation originally developed to predict flooding in packed towers, is selected to predict flooding point:

$$\left[\frac{U_g}{\sqrt{gD}}\left(\frac{\rho_g}{\rho_D}\right)^{1/2}\right]^{2/3}+\frac{1}{2^{1/3}}\left(\frac{G_s/\rho_p}{\sqrt{gD}}\right)^{2/3}=\left(\frac{1}{2\tan\theta}\right)^{1/3} \quad (1)$$

where U_g is the superficial gas velocity, G_s is the solids flux, D the column diameter, θ is the angle of internal friction and is typically around 70 degrees for round-shaped particles.

Equation (2) developed by Bi and Fan [2] based on experimental data in CFB risers is selected to predict the saturation carrying capacity:

$$U_{CA}/\sqrt{gd_p}=21.6Ar^{0.105}(G_s/\rho_g U_{CA})^{0.542} \quad (2)$$

Figure 1 shows such a flow regime diagram for a gas-solids vertical transport line with an upward gas flow. It is seen that there exist five unique flow regimes in the tube, as summarized in Table 1.

Table 1. Flow regimes and corresponding flow patters in a vertical tube with open ends.

Regime	U_g	G_s	Upper section	Lower section
I	$<U_t$	$<G_{s,f}$	Single-phase gas flow	Dilute counter flow
II	$<U_t$	$>G_{s,f}$	Dense co-current flow	Dense counter flow
III	$>U_t$	$<G_s^*$	Dilute co-current flow	Single-phase gas flow
IV	$>U_t$	$G_s^*<G_s<(G_s^*+G_{s,f})$	Dilute co-current flow	Dilute counter flow
V	$>U_t$	$>G_s^*+G_{s,f}$	Dense co-current flow	Dense counter flow

FLOW PATTERNS IN BOTTOM-RESTRICTED CIRCULATING FLUIDIZED BED SYSTEMS

If the bottom of the tube is restrained by a distributor to prevent particles from escaping from the bottom of the system, a circulating fluidized bed forms as shown in Figure 2(b). Thus, two types of flow systems can be distinguished, with the free system corresponding to transport operation as shown in Figure 2(a), while the bottom-restricted system corresponds to (circulating) fluidized bed operation as indicated in Figure 2(b). A circulating fluidized bed can be operated in either a co-current upward flow (pneumatic transport) mode or fast fluidization mode, depending

on the gas velocity and solids circulation rate. It can be visualized that the flow pattern in the bottom-restricted CFB riser should be identical to the upper section above the solids feeding point of a free pneumatic vertical transfer line when the solids feeding/circulating rate is lower than the saturation carrying capacity of the gas. When the solids feeding rate is higher than the saturation carrying capacity, a dense bed forms at the bottom of the riser and develops upward with further increase in the solids feeding rate under steady state operation. The global flow patterns in the riser then resembles the "fast fluidization" as commonly accepted in the literature, with a dense region in the lower section and a dilute region in the upper section of the riser.

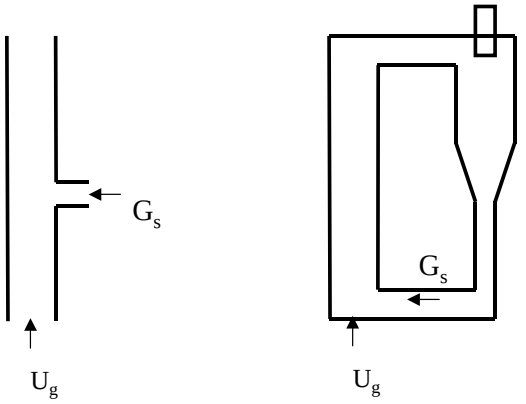

(a) Free system (b) Bottom-restricted

Figure 2. Illustration of (a) free vertical transport system and (b) bottom-restricted CFB system.

A dense fluidized bed is typically operated at the saturation carrying capacity point, with entrainment rate equal to the saturation carrying capacity. The transition from bubbling to turbulent fluidization would thus be better defined by the flow pattern difference in the dense fluidization region. As generally agreed, such a transition corresponds to the balance between bubble coalescence and splitting, as reflected by the maximum pressure fluctuations in the dense bed, denoted by transition velocity U_c. The transition from turbulent fluidization to fast fluidization has still not been well defined. Some considered a critical velocity, U_{se}, corresponding to the onset of significant particle entrainment as the transition form turbulent to fast fluidization [3, 4]. This critical velocity can be considered as a hindered or apparent terminal settling velocity of bed particles, reflecting the existence of particle clusters or agglomerates in the dense fluidized beds for Group A and fine Group B particles. For Group D particles, U_{se} is essentially the same as the terminal settling velocity of single particles. Others proposed a transport velocity, U_{tr}, beyond which the sharp change of vertical pressure drop gradient with increasing solids circulation rate disappears to quantify the transition from turbulent to fast fluidization [5]. An examination of pressure gradient profiles reveals that U_{tr} varies with height. U_{tr} may indicate a transition of axial voidage profiles in the riser [6]. Below this velocity, a distinct interface exists between the top-dilute and bottom-dense regions. Beyond this velocity, the interface becomes relatively diffuse. For Group A powders, another transition velocity, U_k, defined as the level-off point in pressure fluctuations with

further increase in gas velocity, was proposed in early years to represent the disappearance of bubbles in the fluidized bed [5]. Such a transition velocity was not consistently identified in later studies because of the strong influence of solids return system design [4, 7]. Quantitatively, reported U_k values were found to be very close to the critical velocity U_{se} [6], suggesting some linkage between the breakdown of bubbles in the dense bed and the onset of significant entrainment of particles from the dense fluidized bed. If the transition from turbulent fluidization to fast fluidization is considered as corresponding to the flow pattern changes in the dense fluidized beds, e.g. the disappearance of regular shaped bubbles or voids, then such a transition can be demarcated by either U_k or U_{se}. On the other hand, if such a transition is considered as the disappearance of a distinct dense-dilute interface around the upper bed surface, then U_{tr} can be used to demarcate such a transition. Quantitatively, U_{tr} appears to be slightly higher than U_{se} and U_k, but generally around 1 to 2 m/s for Group A powders.

Once substantial solids entrainment occurs at a gas velocity well above the transport velocity, the flow pattern in the CFB riser now depends on not only the superficial gas velocity but also the solids feeding rate, with the standpipe being coupled with the riser to establish a circulation loop. As a result, the circulation rate in the CFB system is now also influenced by the solids inventories due to the global pressure balance over the whole solids circulation loop [8]. Such a pressure balance becomes a key in understanding the "choking" phenomenon defined as the critical condition when the CFB riser terminates its stable operation, either because of the gas blower limitation to support a dense flow in the riser or the insufficient pressure head buildup in the standpipe to feed particles from the standpipe side into the riser due to a lower solids inventory [9], see Figure 3. For an ideal system with no "slugging" in the riser flow, there is no reason that prevents the riser to be operated at a full dense suspension flow at high solids circulation rates when the limitations from the gas blower and the standpipe solids return line are eliminated. The riser can thus be operated in a "dense suspension upflow" regime [10], similar to those identified in Figure 1.

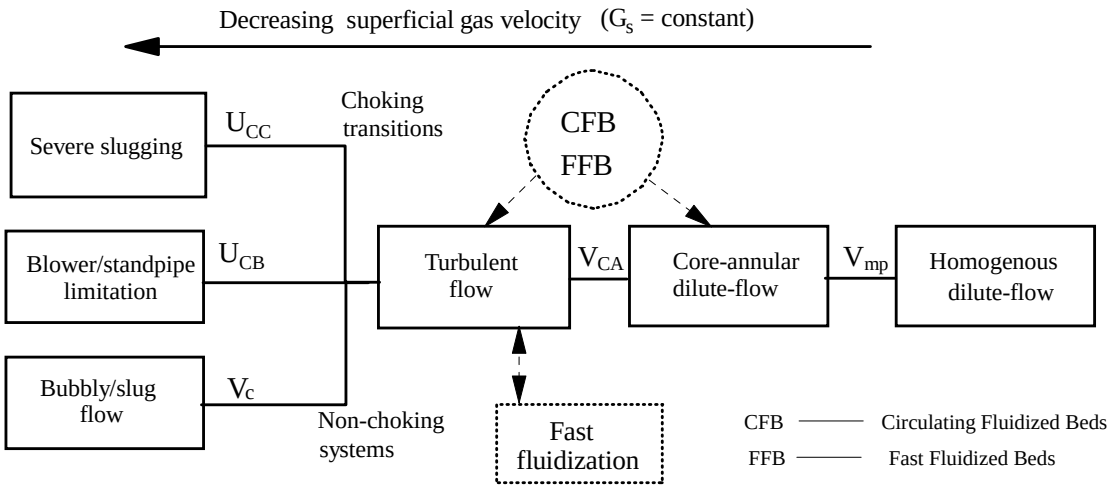

Figure 3. Flow patterns and termination of stable operation in a bottom-restricted CFB system.

FLOW REGIME MAPS FOR BOTTOM-RESTRICTED CIRCULATING FLUIDIZED BEDS

The first attempt concerning the gas-solids co-current upward flow appears to be made by Zenz [11] with the pressure drop over a unit length (dP/dz) plotted versus the superficial gas velocity (Figure 4). He tried to develop a unified flow diagram combining experimental findings from traditional low velocity fluidized beds and pneumatic transport lines. The co-current gas-solids flow region in the diagram spans the flow regimes encountered in the circulating fluidized beds with the lower limit set by the “choking” velocity. The lower velocity fluidization is divided into a "dense phase" fluidization (likely to correspond to the bubbling fluidization) and "turbulent" fluidization (may be the same as the slugging/turbulent fluidization used nowadays) regions. The missing linkage between the lower velocity fluidization and the co-current upflow was attributed to “choking”. Such a regime diagram has been further extended to incorporate more sub-regions for the co-current upflow [12], including at least the homogeneous dispersed flow, core-annulus flow and fast fluidization. Since the pressure gradient (dP/dz) is proportional to the solids fraction if the friction and acceleration/deceleration are neglected, one can alternatively plot solids fraction [13] or bed voidage [3, 14] versus the superficial gas velocity (U) or the normalized superficial gas velocity (U/v_t).

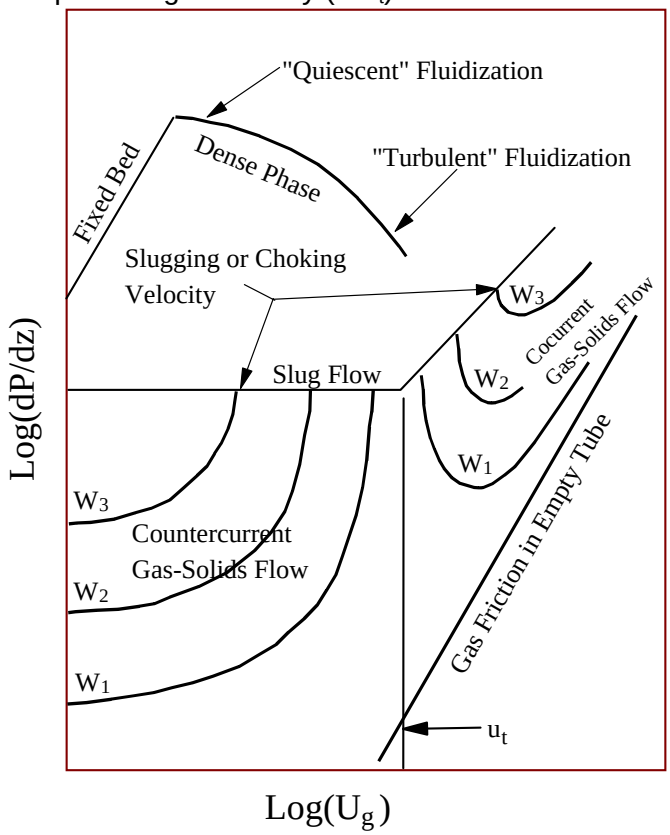

Figure 4. Flow regime diagram of Zenz (1949) for both free and bottom-restricted vertical transport lines. W is the solid flux rate and u_t is the terminal velocity.

Another group of diagrams plots solids circulation rate (G_s) or solids loading ratio [$G_s/(\rho_g U)$] versus the superficial gas velocity or normalized superficial gas velocity, with one typical diagram shown in Figure 5. It is seen that the flow patterns in CFB

riser could be divided into the dilute phase flow, refluxing flow, fast fluidization and, ideally, turbulent and bubbly flow regimes if the severe slugging and blower and standpipe limitations are absent.

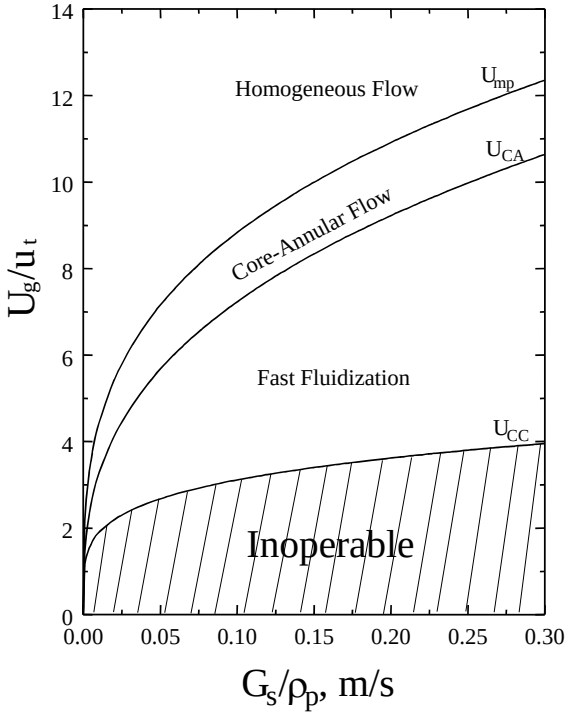

Figure 5. Flow regime diagram for co-current upward bottom-restricted CFB risers [12].

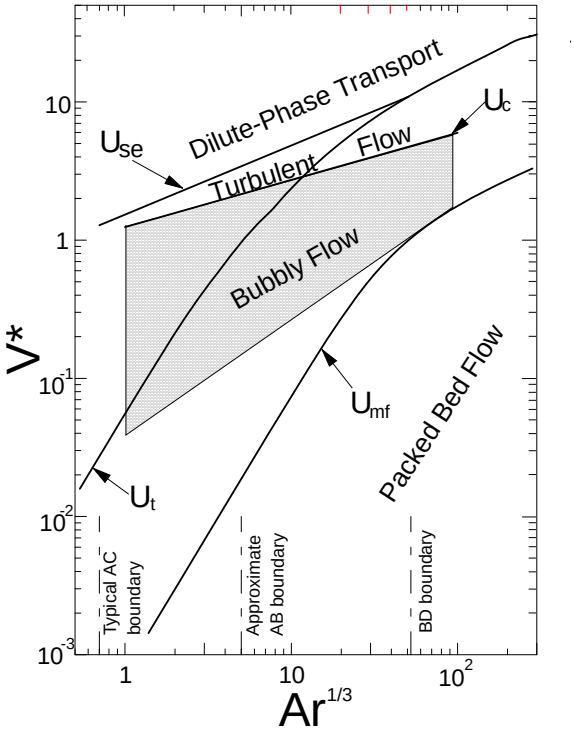

Figure 6. An ideal flow regime map for both fluidized beds and co-current upflow risers [12]. V* is the relative velocity between the superficial gas and particle velocities.

Grace [15] incorporated the typical operation regions of pneumatic transport lines and fast fluidized beds into a phase diagram plotted with the dimensionless superficial gas velocity versus the dimensionless particle diameter. The typical operation region for bubbling fluidized beds and the spouted beds are also identified in this diagram. Bi and Grace [12] extended this diagram by plotting the dimensionless relative velocity between the gas and particles against the dimensionless particle diameter, see Figure 6. Such a diagram is thus believed to be able to identify the ideal flow regimes without the solids circulation rate G_s provided in the diagram by assuming that the flow pattern will be primarily determined by the relative motion between the gas and particles in co-current upflow systems.

To summarize, each diagram has its particular use and advantages. Those developed by Grace [15] and others mostly apply to dense fluidized beds with limited solids entrainment/circulation. The other two types of diagrams developed for vertical upflow in the riser, on the other hand, can provide detail quantitative boundaries between flow regimes for each riser-particle-gas system. The one developed by Bi and Grace [12] attempted to extend the Grace [15] diagram to the vertical co-current upflow riser system, without considering the limitations from the blower/standpipe.

Therefore, the severe slugging, blower and standpipe limitations are not captured in almost all of these ideal phase diagrams, but can be identified by using appropriate analyses and approaches as demonstrated in [8] for specific CFB systems.

CONCLUSION

A flow regime diagram for the non-restricted vertical transport lines includes at least 5 different flow patterns in the riser below and above the solids feeding level, with flooding limiting the maximum solids downflow through the lower section and saturation carrying capacity limiting the upward solids flow rate. In a bottom-restricted CFB riser, the same flow patterns exist in the upper section, except that there are now no particles leaving the riser from the bottom of the riser. The coupling of the riser and the standpipe makes the maximum solids circulation rate now being determined by the pressure balance over the whole CFB loop and the capability of the standpipe and the gas blower to withstand pressure fluctuations induced by severe slugging in the riser for slugging systems.

REFERENCES

1. Papa, G.; Zenz, F. A. Optimize performance of fluidized-bed reactors. Chem. Eng. Prog. 1995, 91(4), 32.
2. Bi HT, Fan LS. Regime transitions in gas-solid circulating fluidized beds. Paper #101e, AIChE Annual Meeting, Los Angeles, Nov. 17-22, 1991.
3. Li Y, Kwauk M. The dynamics of fast fluidization. In: Grace JR, Matsen JM, eds. Fluidization. New York: Plenum, 1980, pp.537-544.
4. Bi HT, Grace JR, Zhu JX. Regime transitions affecting gas-solids suspensions and fluidized beds. Chem Eng Res Des 73:154-161, 1995.
5. Yerushalmi J, Cankurt NT. Further studies of the regimes of fluidization. Powder Technol 24:187-205, 1979.
6. Bi, H.T., Transition from turbulent to fast fluidization, Chem. Eng. Comm., 189, 942-958, 2002.
7. Rhodes, M.J. and D. Geldart, Transition to turbulence? Fluidization V, K. Ostergaard and A. Sorensen eds., Science Foundation, New York, pp.281-288, 1986.
8. Bi HT, Zhu JX. Static instability analysis of circulating fluidized beds and the concept of high-density risers. AIChE J 39:1272-1280, 1993.
9. Bi HT, Grace JR, Zhu JX. On types of choking in pneumatic systems. Int J Multiphase Flow 19:1077-1092, 1993.
10. Grace JR, Issangya AS, Bai DR, Bi HT, Zhu JX. Situating the high-density circulating fluidized beds. AIChE J 45:2108-2116, 1999.
11. Zenz FA. Two-phase fluidized-solid flow. Ind Eng Chem 41:2801-2806, 1949.
12. Bi HT, Grace JR. Flow regime maps for gas-solids fluidization and upward transport. Int J Multiphase Flow, 21:1229-1236, 1995.
13. Squires, A.M., M. Kwauk and A.A. Avidan, Fluid beds: at last, challenging two entrenched practices, Science, 230, 1329-1337, 1985.
14. Avidan, A.A. and J. Yerushalmi, Bed expansion in high velocity fluidization, Powder Technol., **32**, 223-232, 1982.
15. Grace JR. Contacting modes and behaviour classification of gas-solid and other two-phase suspensions. Can J Chem Eng 64:353-363, 1986.